

Supporting Information

Compartmentalization and Unidirectional Cross-Domain Molecule Shuttling of Organometallic Single-Chain Nanoparticles

Zhigang Cui, Leilei Huang, Yi Ding, Xuechao Zhu, Xinhua Lu, Yuanli Cai*

State-Local Joint Engineering Laboratory of Novel Functional Polymeric Materials, College of Chemistry, Chemical Engineering and Materials Science, Soochow University, Suzhou 215123, China

Characterization. *UV-Vis Spectroscopy* was performed using a Shimadzu UV-3600 spectrometer. Intermediate thiol protection was confirmed using Ellman method.¹ Ellman reagent was prepared by dissolving 5, 5'-dithiobis-2-nitrobenzoic acid in 0.1 M phosphate buffer (0.4 mg/mL, pH 8.0). Polymer (**P-2**, Figure S1; 4.0 mg) was dissolved in phosphate buffer (2.0 mL). Solution was bubbled with argon gas for 1 h. Ellman reagent (50 μ L) was added. The solution was stirred for 10 min before UV-vis spectroscopy. *¹H NMR Spectroscopy* was conducted on a Unity INOVA 400NB NMR spectrometer. *Size Exclusion Chromatography (SEC)* was conducted on a PL-GPC220 integrated 3 system with RI detector and a set of columns (2 \times PLGel MIXED-B+1 \times PLGel MIXED-D). PMMA standards (Agilent, 1.95–1048 kDa) were used for calibration. The calibration and analysis proceeded using DMF eluent that contained 10.0 mM LiBr at a 1.0 mL/min flow rate at 80°C. NH_3^+ and imidazolium-motifs were converted into nonionic derivatives by reaction with di-*tert*-butyldicarbonate in the presence of triethylamine in methanol at room temperature for 3 days. The solution was filtered using a 200 nm filter prior to SEC measurement. *Dynamic Light Scattering (DLS)* was performed on a Brookhaven BI-200SM setup equipped with 35-mW He-Ne laser, BI-200SM goniometer and BI-TurboCorr digital correlator. Temperature was fixed at 25°C using a BI-TCD controller. Dusts were removed using a 200-nm syringe filter. Sample was measured at an angle of 90°. Number-average hydrodynamic diameter ($D_{h, \text{DLS}}$) was determined by cumulants analysis in CONTIN routine. Data were averaged over 5 runs. *NMR Diffusion-Ordered Spectroscopy (DOSY)* was conducted on an Agilent direct-Drive II 600MHz NMR spectrometer using a 5 mm OnNMR probe and a gradient amplifier, fulfilled in a Dbppste-cc pulse sequence with z-direction gradient strength to 60 G/cm at 25°C. Proton pulse length was 8.9 μ s. Gradient length was set to 2 ms and gradient strength was incremented over 1.13–28.26 G/cm in 15 steps, scanning for 128 times. Gradient recovery delay time was set to 1 s at acquisition time of 1.7 s. The diffusion delay (Δ) was set to 400 ms. Diffusion coefficient (D) was analyzed using a Vnmrj3.2 software, using the signal $\text{CH}(\text{OH})\text{CH}_3$ of PHPMA as calibration standard. The mean hydrodynamic diameter ($D_{h, \text{DOSY}}$) was calculated using Stokes-Einstein Equation, $D_{h, \text{DOSY}} = kT/3\pi\eta D$, in which k is Boltzmann constant, T is solution temperature, and η is solvent viscosity (D_2O : 1.100×10^{-3} Pa s).² *Aqueous Electrophoresis* was performed on a Malvern Zetasizer Nano-ZS90 instrument. *Transmission Electron Microscopy (TEM)* was performed on a Hitachi HT7700 transmission electron microscope at an accelerating voltage of 120 kV. Sample was prepared by diluting solution to 0.5 mg/mL. 10 μ L aliquot was dripped onto the copper grid, deeply frozen using liquid nitrogen, and dried under reduced pressure. Number-weighted diameter (D_n) was determined by statistical analysis from >500 particles, using a Nano Measurer 1.2 software. *Fourier Transform Infrared (FTIR)* spectra of **SCNP-1** and **SCNP-2** were recorded on a Nicolet 6700 spectrometer. Samples were prepared by freeze-drying in a Labconco Freezone2.5L freeze-drier prior to FTIR measurements.

Materials. Block copolymers, PHisAM₅₈-*b*-PHPMA₅₇-*b*-PAEMA₅₈ (¹H NMR: M_n = 29.6 kDa; SEC: M_n = 24.9 kDa, \bar{D} = 1.09), PHPMA₅₅-*b*-PAEMA₅₇ (¹H NMR: M_n = 17.5 kDa; SEC: M_n = 19.3 kDa, \bar{D} = 1.07) and PHPMA₆₀-*b*-PHisAM₅₆ (¹H NMR: M_n = 20.1 kDa; SEC: M_n = 16.9 kDa, \bar{D} = 1.09) were synthesized via visible light mediated RAFT polymerization reported elsewhere.³ 2-Hydroxyethyl acrylate (HEA), dimethylphenylphosphine (Me_2PPh) were purchased from Sigma-Aldrich; deuterium oxide (D_2O , 99.8% D), sodium deuterioxide (99.5% D, 40% in D_2O) and deuterchloric acid (99.5% D, 20% in D_2O) from J&K; ascorbic acid (AA), CuCl_2 and other reagents from Aladdin. These reagents were used as received. Deionized water (>18.2 M Ω /cm) was obtained from a Direct-Q 5 UV Millipore system, and used for the synthesis and characterization.

End-Group Protection. PHisAM₅₈-*b*-PHPMA₅₇-*b*-PAEMA₅₈ (**P-1**; 0.85 g, 28.7 μ mol trithiocarbonate, TTC) was dissolved in methanol/water mixture (2:8, w/w; 4.0 g). The solution was adjusted to pH 10.0, bubbled with argon for 40 min, and stirred at 25°C overnight. Sample (0.5 mL) was taken, dialyzed against water at pH 2.5, and freeze-dried as the intermediate polymer, **P-2**. The solution was acidified to pH 3.5. HEA (0.17 g, 1.44 mmol) and Me_2PPh (7.9 mg, 57.4 μ mol) were added. Solution was stirred at 25°C for 24 h, dialyzed against water at pH 2.5, and freeze-dried to afford the final product, **P-3**. Yield: 0.72 g, 85%. Figure S1a shows that the bands at $\lambda_{\text{max, TTC}} = 304$ nm and $\lambda_{\text{max, SH}} = 408$ nm (*inset*) disappeared. End-group protection was confirmed by ¹H NMR spectroscopy (Figure S1b), and >99% conv. was determined using Eq. S1. Quantification using Eqs. S2–S4 confirmed that the polymer kept unchanged. Figure S1c shows that SEC traces are identi-

cal at $M_n = 24.8$ kDa and $\bar{D} = 1.12$. These confirmed successful preparation of well-defined and end-group protected $A_{58}B_{57}C_{58}$ triblock copolymer.

$$\text{Conversion} = \frac{I_{u+v}}{I_{x+y}} \times 100\% \quad (S1)$$

$$DP_{PHisAM} = 2 \times \frac{I_{m+p+q} - I_{x+y}}{I_{x+y}} \quad (S2)$$

$$DP_{PHPMA} = 4 \times \frac{I_h}{I_{x+y}} \quad (S3)$$

$$DP_{PAEMA} = \frac{I_{c+l} - I_{m+p+q} + I_{x+y}}{I_{x+y}} \quad (S4)$$

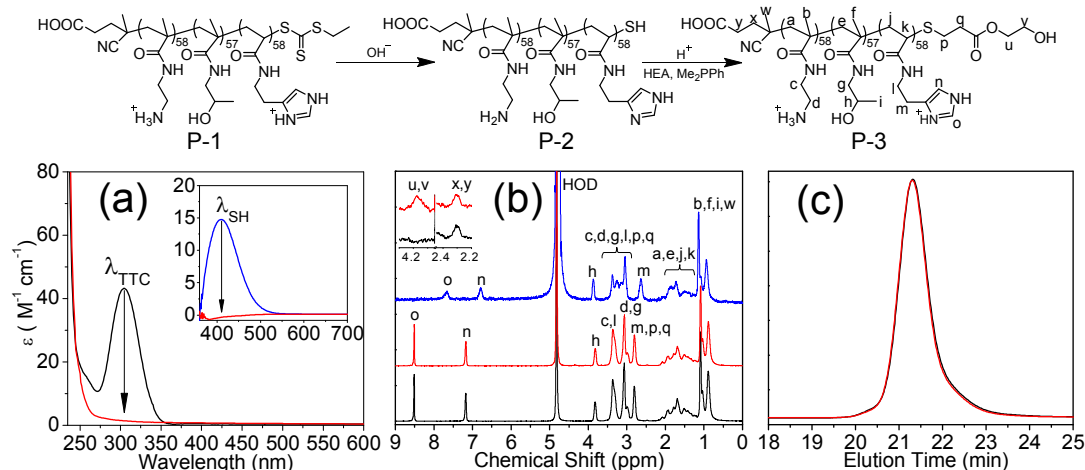


Figure S1. Schematic illustration of end-group protection. (a) UV-vis spectra of **P-1** (black), **P-3** (red); inset: Ellman solutions of **P-2** (blue), **P-3** (red). (b) ^1H NMR spectra of **P-1** (black), **P-3** at pH 2.5 (red), 6.4 (blue). (c) SEC traces of **P-1** (black), **P-3** (red).

Preparation of Dumbbell-Shape SCNP-1. Briefly, **P-3** (0.300 g, 1.17 mmol HisAM + AEMA) and CuCl_2 (50 mg, 0.29 mmol) were dissolved in 150 mL water. The solution was acidified at pH 2.5, and neutralized stepwise to pH 6.4 using 0.5 M NaOH. The solution was stirred at room temperature overnight. Sample was taken and analyzed using UV-vis spectroscopy, FTIR, ^1H NMR, DOSY, DLS, and TEM.

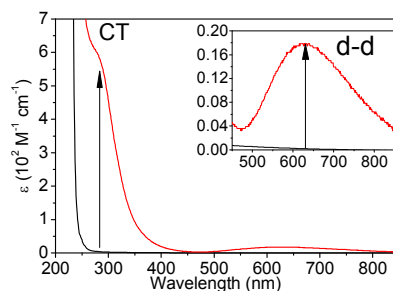


Figure S2. UV-vis spectra of the **P-3** solutions at $[\text{Cu(II)}]/[\text{ligands}] = 1/4$, pH 2.5 (black) and 6.4 (red).

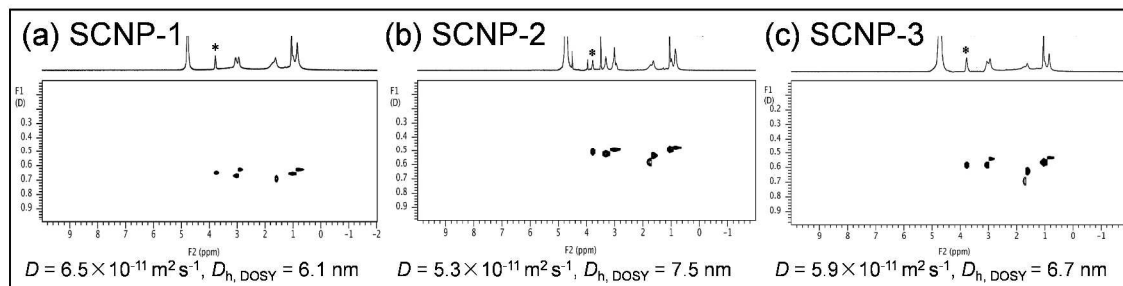


Figure S3. DOSY spectra of (a) **SCNP-1**, (b) **SCNP-2** prepared by the reduction of **SCNP-1** at $f=2.0$, and (c) **SCNP-3** prepared by air oxidation of **SCNP-2**. Herein, D and $D_{h,DOSY}$ are diffusion coefficient and mean hydrodynamic diameter, respectively.

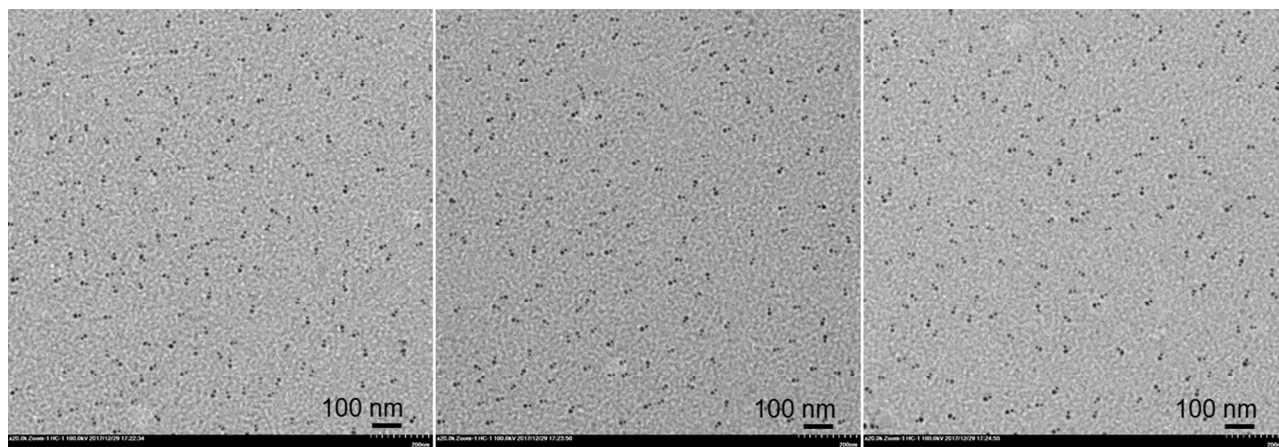


Figure S4. TEM images of **SCNP-1**, which clearly display the discrete double heads. Statistical analysis from >500 particles, using a Nano Measurer 1.2 software, indicated the D_n values of 13.6 and 9.4 nm of these discrete double heads.

Ascorbic Acid Reduction of SCNP-1. Typically, the argon-saturated AA solution (3.0 w/w%, 0, 12.9, 25.7, 38.6, 51.5 mg; 0, 2.0, 4.0, 5.8, 7.8 μ mol AA) was added into the argon-saturated **SCNP-1** solution (2.0 mg/mL, 2.0 mL; 3.9 μ mol copper ions). The solution was adjusted to pH 6.4, bubbled with argon for 45 min, and stirred at 25°C overnight. Sample was analyzed with UV-vis spectroscopy, FTIR, ^1H NMR, DOSY, DLS, and TEM.

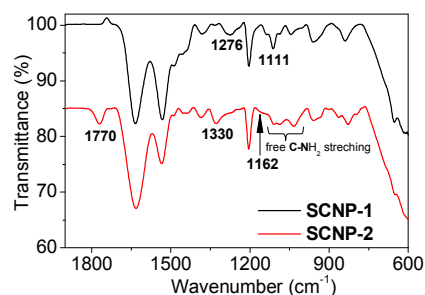


Figure S5. FTIR spectra of dried **SCNP-1** (black) and **SCNP-2** (red). Cu(II)-imidazole's C=N ring stretching vibration⁴ at 1276 cm^{-1} (**SCNP-1**) upshifted to 1330 cm^{-1} [Cu(I)-imidazole's C=N ring stretching vibration⁵ in **SCNP-2**], suggesting the conversion of Cu(II)-imidazole into Cu(I)-imidazole. Moreover, Cu(II)-NH₂ complex C-N stretching⁶ at 1111 cm^{-1} (**SCNP-1**) disappeared and Cu(I)-NH₂ complex's C-N stretching⁷ at 1162 cm^{-1} is unobservable in **SCNP-2**, and the C-N stretching⁶ of free alkyl-NH₂ in **SCNP-2** is observed. These results suggest that C-block's NH₂-ligands in **SCNP-2** have been dissociated. In addition, ascorbic acid C=O stretching⁸ at 1770 cm^{-1} was observed in **SCNP-2**. These results confirmed that **SCNP-1**'s Cu(II)-ligands converted into solely Cu(I)-imidazole complex in **SCNP-2**. That is, C-block disassembled and A-block reassembled upon the metal reduction at $f = 2.0$.

The fraction of unfolded C-block (PAEMA%) was determined by ^1H NMR studies using Eq. S5, where $I_{3.4}$, $I_{3.9}$ are integral signals $\text{CONHCH}_2\text{CH}_2\text{NH}_3^+$ of AEMA unit at $\lambda = 3.4$ ppm, $\text{CH}(\text{OH})\text{CH}_3$ of HPMA unit at 3.9 ppm (Figure 2B), respectively.

$$\text{PAEMA}\% = \frac{I_{3.4}}{2 \times I_{3.9}} \times \frac{DP_{\text{HPMA}}}{DP_{\text{PAEMA}}} \times 100\% \quad (\text{S5})$$

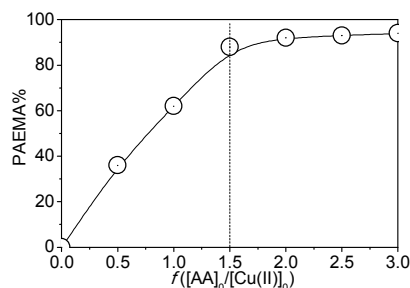


Figure S6. The variation of unfolded C-segmental fraction (PAEMA%) upon reduction with AA at different f values.

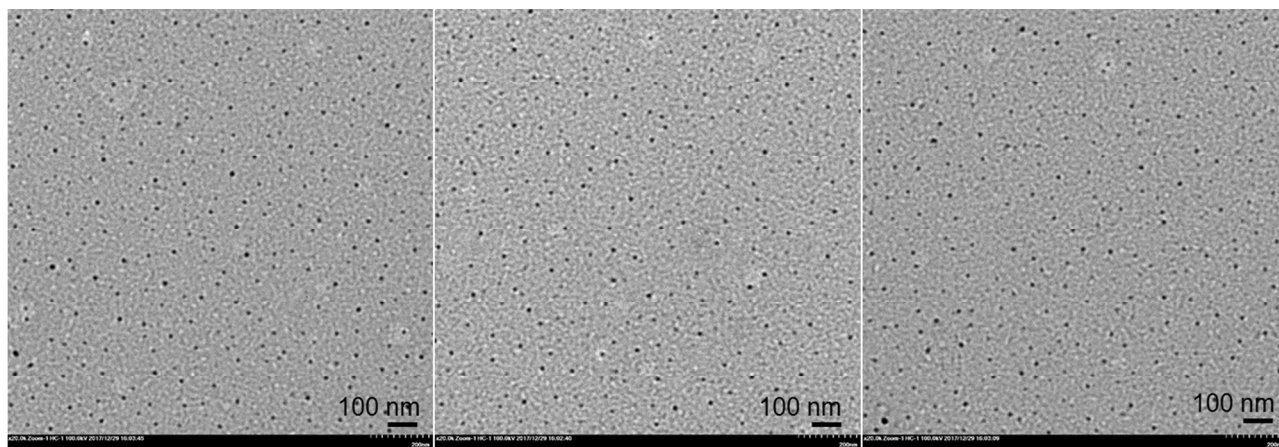


Figure S7. TEM images of SCNPs prepared by reduction of SCNPs at $f = 2.0$, which confirmed the spherical shape of as-formed SCNPs. Statistical analysis from >500 particles using a Nano Measurer 1.2 software indicated a D_n value of 15.6 nm.

Ascorbic Acid Reduction of Diblock Copolymer Cu(II)-SCNPs. PHPMA₆₀-*b*-PHisAM₅₆ (0.10 g, 0.28 mmol HisAM), CuCl₂ (11.8 mg, 69 μmol) were dissolved in 50 mL water. Solution was acidified to pH 2.5 and then neutralized to pH 6.4 to yield Cu(II)-SCNP. AA (3.0 w/w%, 183 mg; 27.7 μmol) was added into the solution (5.0 mL, 7.0 μmol copper). The solution was adjusted to pH 6.4, bubbled with argon gas for 45 min, and stirred at 25°C overnight to yield Cu(I)-SCNP. AA-reduction of Cu(II)-SCNPs of PHPMA₅₅-*b*-PAEMA₅₇ proceeded under the same conditions except using PHPMA₅₅-*b*-PAEMA₅₇ copolymer.

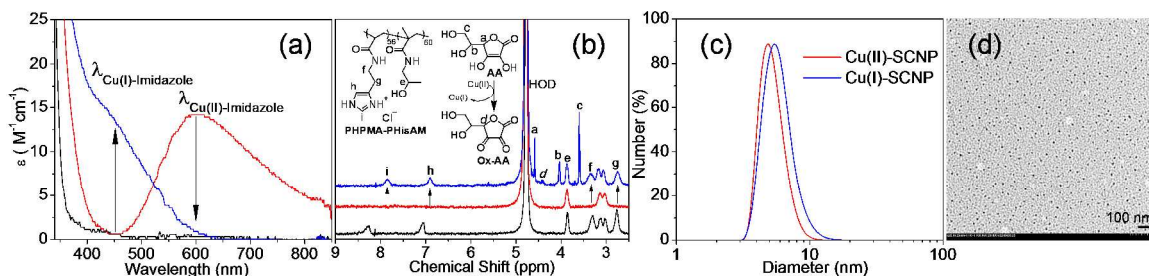


Figure S8. (a) UV-vis and (b) ¹H NMR spectra of PHPMA₆₀-*b*-PHisAM₅₆ (black), the Cu(II)-SCNP (red) and Cu(I)-SCNP (blue). (c) DLS diameter profiles of SCNPs. (d) TEM image of Cu(I)-SCNP. Based on the ¹H NMR studies using Eqs. S6-S8, 53% PHisAM segments unfolded, 54% AA (F_{AA}) retained, and only 5% of as-generated Ox-AA (F_{Ox-AA}) are detectable.

$$PHisAM\% = \frac{I_g}{2 \times I_e} \times \frac{DP_{PHPMA}}{DP_{PHisAM}} \times 100\% \quad (S6)$$

$$F_{AA} = 2 \times \frac{I_c}{I_e} \times \frac{DP_{PHPMA}}{DP_{PHisAM}} \times \frac{[Cu(II)]_0}{[AA]_0} \times 100\% \quad (S7)$$

$$F_{Ox-AA} = 4 \times \frac{I_d}{I_e} \times \frac{DP_{PHPMA}}{DP_{PHisAM}} \times \frac{[Cu(II)]_0}{[AA]_0} \times 100\% \quad (S8)$$

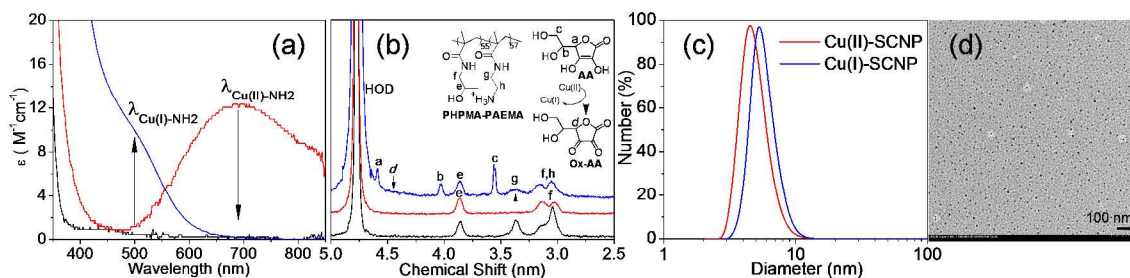


Figure S9. (a) UV-vis and (b) ¹H NMR spectra of PHPMA₅₅-*b*-PAEMA₅₇ (black), the Cu(II)-SCNP (red) and Cu(I)-SCNP (blue). (c) DLS diameter profiles of SCNPs. (d) TEM image of Cu(I)-SCNP. Based on ¹H NMR studies using Eqs. S9, S10, 52% PAEMA segments unfolded and 54% AA (F_{AA}) retained. Figure S9b shows that Ox-AA signal *d* disappeared, suggesting full encapsulation of Ox-AA into as-reassembled heads.

$$PAEMA\% = \frac{I_g}{2 \times I_e} \times \frac{DP_{PHPMA}}{DP_{PAEMA}} \times 100\% \quad (S9)$$

$$F_{AA} = 2 \times \frac{I_c}{I_e} \times \frac{DP_{PHPMA}}{DP_{PAEMA}} \times \frac{[Cu(II)]_0}{[AA]_0} \times 100\% \quad (S10)$$

Air Oxidation of SCNP-2. SCNP-2 solution was bubbled with fresh air at 8-10 bubbles/min at 25°C overnight. Fresh air was obtained by removal of CO₂ and water vapor *via* passing through an anhydrous KOH column. Sample was taken and analyzed with UV-vis spectroscopy, ¹H NMR, DOSY, DLS, TEM, and aqueous electrophoresis.

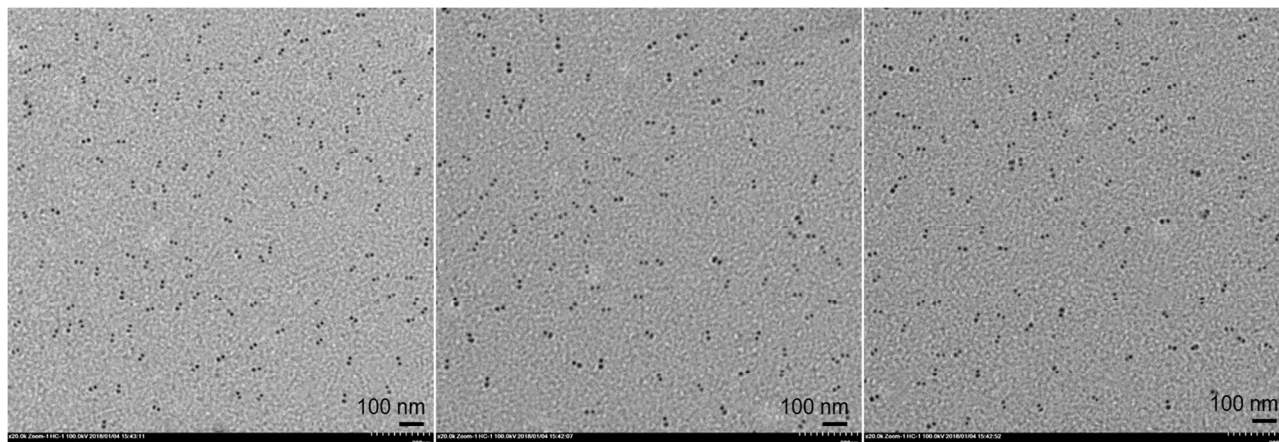


Figure S10. TEM images of SCNP-3 prepared by air oxidation of SCNP-2 at pH 6.4 overnight, which clearly display their discrete double heads. Statistical analysis from >500 particles indicated the D_n values of 15.5 and 12.6 nm of the discrete double heads.

Salting-Out Effect. This effect was confirmed by comparing **Particle I**, formed by addition of NaCl into SCNP-2 solution, with **Particle II**, formed by addition of AA (equal molar to aforementioned NaCl) into SCNP-1 solution. Briefly, **Particle I** was prepared by adding the argon-saturated NaCl solution (1.76 M, 13 μ L; 23.4 μ mol) into argon-saturated SCNP-2 solution (2.0 mL, 3.9 μ mol copper ions; [NaCl]/[Cu(I)] = 6.0). **Particle II** was prepared by adding the argon-saturated AA solution (3.0 w/w%, 184 mg; 31.3 μ mol AA) into the argon-saturated solution of SCNP-1 solution (2.0 mL; 3.9 μ mol copper centers; f = 8.0). These solutions were adjusted to pH 6.4 and stirred at 25°C overnight prior to the measurements.

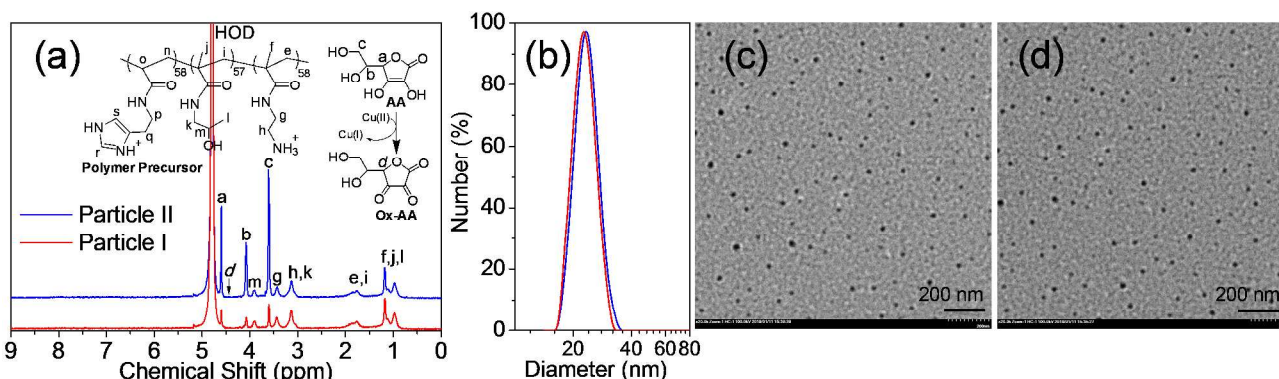


Figure S11. (a) ¹H NMR spectra and (b) DLS diameter profiles of **Particle I** (red) and **Particle II** (blue). TEM images of (c) **Particle I** and (d) **Particle II**.

Figure S11a indicates that, in both cases, A-segments collapsed, C-segments unfolded, and Ox-AA has been encapsulated. DLS and TEM studies confirmed comparable size distributions of these spherical nanoparticles (**Particle I**: $D_{h,DLS}$ = 19.1 nm, D_n = 24.1 nm; **Particle II**: $D_{h,DLS}$ = 19.4 nm, D_n = 24.6 nm). These results confirmed that the unreacted AA played electrolyte role, which brought about salting-out effect that could induce the undesired intermolecular self-assembly.

REFERENCES

- (1) Qiu, X. P.; Winnik, F. M. Facile and Efficient One-Pot Transformation of RAFT Polymer End Groups via a Mild Aminolysis/Michael Addition Sequence. *Macromol. Rapid Commun.* **2006**, *27*, 1648-1653.
- (2) Cho, C. H.; Urquidi, J.; Singh, S.; Robinson, G. W. Thermal Offset Viscosities of Liquid H₂O, D₂O, and T₂O. *J. Phys. Chem. B* **1999**, *103*, 1991-1994.
- (3) Cui, Z.; Cao, H.; Ding, Y.; Gao, P.; Lu, X.; Cai, Y. Compartmentalization of An ABC Triblock Copolymer Single-Chain Nanoparticle via Coordination-Driven Orthogonal Self-Assembly. *Polym. Chem.* **2017**, *8*, 3755-3763.
- (4) Materazzi, S.; Vecchio, S.; Wo, L. W.; Curtis, S. D. A. TG-MS and TG-FTIR Studies of Imidazole-Substituted Coordination Compounds: Co(II) and Ni(II)-Complexes of Bis(1-methylimidazol-2-yl)ketone. *Thermochim. Acta* **2012**, *543*, 183-187.

- (5) Pelli, M.; Gandin, V.; Marzano, C.; Marinelli, M.; Del Bello, F.; Santini, C. The First Water-Soluble Copper(I) Complexes Bearing Sulfonated Imidazole- and Benzimidazole-Derived N-Heterocyclic Carbenes: Synthesis and Anticancer Studies. *Appl. Organomet. Chem.* DOI: 10.1002/aoc.4185.
- (6) Sen, D. N.; Mizushima, S.; Curran, C.; Quagliano, J. V. Infrared Absorption Spectra of Inorganic Coordination Complexes. 1. the Nature of Chelation Bonding in Bis-(glycino)-copper(II) Monohydrate and Bis-(glycino)-nickel(II) Dihydrate. *J. Am. Chem. Soc.* **1955**, 77, 211-212.
- (7) Aripomammal, S.; Chandrasekaran, S.; Sanjeeviraja, C. Low Temperature Photoluminescence Studies on Semiorganic Tris Thiourea Copper (I) Chloride Single Crystal. *Cryst. Res. Technol.* **2012**, 47, 145-150.
- (8) Sk, M. M.; Yue, C. Y. Synthesis of Polyaniline Nanotubes Using the Self-Assembly Behavior of Vitamin C: a Mechanistic Study and Application in Electrochemical Supercapacitors. *J. Mater. Chem. A* **2014**, 2, 2830-2838.